Molecular Electronics

Deutsche Ausgabe: DOI: 10.1002/ange.201604748
Internationale Ausgabe: DOI: 10.1002/anie.201604748

Gradients of Rectification: Tuning Molecular Electronic Devices by the Controlled Use of Different-Sized Diluents in Heterogeneous Self-Assembled Monolayers

*Gyu Don Kong, Miso Kim, Soo Jin Cho, and Hyo Jae Yoon**

Abstract: *Molecular electronics has received significant attention in the last decades. To hone performance of devices, eliminating structural defects in molecular components inside devices is usually needed. We herein demonstrate this problem can be turned into a strength for modulating the performance of devices. We show the systematic dilution of a monolayer of an organic rectifier (2,2′-bipyridine-terminated n-undecanethiolate) with electronically inactive diluents (n-alkanethiolates of different lengths), gives remarkable gradients of rectification. Rectification is finely tunable in a range of approximately two orders of magnitude, retaining its polarity. Trends of rectification against the length of the diluent indicate the gradient of rectification is extremely sensitive to the molecular structure of the diluent. Further studies reveal that noncovalent intermolecular interactions within monolayers likely leads to gradients of structural defect and rectification.*

Structural defects in molecular components matter in the performance of molecular- and nano-electronic devices.[1] For achieving high yielding and great functioning electronic devices, it is usually required to eliminate or minimize structural defects in electronically active components. However, how structural defects in molecular components influence the device performance, and how such an influence is related to the molecular structure of the additive that causes the structural defects remain uncertain. If these challenging issues can be resolved, it would turn the problem caused by structural defects into a useful means to modulate the performance of device by controlling the structure of the additive and its content ratio inside a device.

We describe herein a model study to investigate electrical behavior of self-assembled monolayer (SAM)-based large area molecular junctions as a function of heterogeneity of the monolayer. Well-defined binary SAMs of organic rectifier (2,2′-bipyridyl *n*-undecanethiol; denoted as $HSC_{11}BIPY$) and non-rectifying diluents (*n*-alkanethiol; denoted as HSC_n) were electrically characterized using Ga_2O_3/EGaIn conical microelectrodes (Ga_2O_3/EGaIn is eutectic gallium-indium alloy covered with a self-passivating Ga_2O_3 film).[2] We found that the magnitude of rectification ratio can be finely controlled, in a range of approximately two orders of magnitude, through control over the ratio of diluent to rectifier within the monolayer, while retaining the polarity of rectification. Furthermore, we established molecular scaling over the diluents: structural difference (in this case, by length) between diluent and rectifier determines the gradients of rectification.

For examining electrical characteristics of heterogeneous SAMs, this study focused on rectification. Rectification is an early justification for the field of molecular electronics.[3] Rectification [r; Eq. (1)] is a self-referencing parameter.

$$r = |J(+V)|/|J(-V)| \quad (1)$$

It is estimated by the ratio of current densities ($J(V)$; J at applied bias V; $A\,cm^{-2}$) measured at opposite polarities of applied bias on single junction: that is, $J(+V)$ and $J(-V)$ are measured on the same SAM, electrodes, and SAM-electrode interfaces. This feature allows one to eliminate complexities arising from J–V measurements in one bias, and makes rectification particularly attractive to investigate structure–property relations in molecular electronics. Indeed, dispersion of rectification histograms is usually narrower than that of current density histograms since rectification histograms are insignificantly influenced by junction-to-junction variations.[4]

We utilized $HSC_{11}BIPY$ rectifier for this work. Incorporating 4′-methyl-2,2′-bipyridyl moiety (BIPY), which could undergo a single-electron reduction, to a terminus of *n*-alkanethiolate leads to significant r values with high reproducibility. Rationale concerning the design of this molecule has been documented in detail elsewhere.[5] Molecular junctions of the form, $Ag^{TS}/SC_{11}BIPY//Ga_2O_3$/EGaIn (where Ag^{TS} is template-stripped silver substrate)[6] exhibit high yields of working junctions ($\geq$ ca.70%) and statistically significant r (mean of r, $|r|_{mean} \approx 85$) with a narrow dispersion (standard deviation of r, $\sigma_r \approx 2.0$) at ± 1.0 V.[5] The histogram of r values approximately fits a Gaussian curve, from which the mean and standard deviation are extracted. It is believed that the rectification of $SC_{11}BIPY$ SAM stems from different regimes of charge transport at applied biases of opposite polarities ($+V$ and $-V$). Namely, while pure tunneling occurs across the SAM at $-V$, the energy level (LUMO) of the BIPY is coupled with the Fermi level of Ga_2O_3/EGaIn electrode at $+V$, and leads to tunneling followed by hopping.[5,7] Indeed, the experimentally estimated LUMO of the BIPY was approximately 3.7 eV, which is in close proximity to the Fermi level (ca. 4.3 eV) of Ga_2O_3/EGaIn electrode (see the Supporting Information for experimental details on the estimation of LUMO level of BIPY, and the energy diagram of junction).

[*] G. D. Kong, M. Kim, S. J. Cho, Prof. H. J. Yoon
Department of Chemistry
Korea University
Seoul 136-701 (Korea)
E-mail: hyoon@korea.ac.kr

Supporting information for this article can be found under: http://dx.doi.org/10.1002/anie.201604748.

The difference in the regime of charge transport at $+V$ and $-V$ results in asymmetric widths of tunneling barrier for $+V$ and $-V$, thereby leading to different $J(+V)$ and $J(-V)$ values and rectification.

Binary SAMs with *n*-alkyl backbones often exhibit distinct structural features from those of single-component SAMs. Differences in noncovalent interactions between different thiol species result in phase separation and/or defects upon formation of heterogeneous monolayers.[8] For governing lateral interactions within monolayers, several types of intermolecular forces have been introduced.[9] Some of these include intermolecular hydrogen bonds;[8a,10] electrostatic interactions between dipolar moieties;[11] and control of van der Waals (vdW) interactions between *n*-alkyl chains.[12] For this study, the vdW-based strategy was employed to change the supramolecular structure of monolayers because it avoids loss of rectification ratio resulting from additional structural modification of $HSC_{11}BIPY$. The chain length of diluent (HSC_n) was varied while keeping the length of rectifier ($HSC_{11}BIPY$) constant.

To form binary SAMs, solutions containing two different thiols were prepared by mixing 3 mM toluene solutions (degassed by N_2 bubbling) of $HSC_{11}BIPY$ and HSC_n at a desired ratio while the total concentrations were kept at 3 mM. Ag^{TS} chips were immersed in the mixed thiol solutions for 3 h under N_2 atmosphere at room temperature, followed by rinsing with pure toluene and drying in air (see the Supporting Information for detailed procedures). The composition of the binary SAMs was changed by varying the ratio ($\chi^{soln}_{HSC11BIPY} = [HSC_{11}BIPY]/([HSC_{11}BIPY] + [HSC_n])$) of $HSC_{11}BIPY$ and HSC_n in solution from 0.0 to 1.0, where [A] (A = HSC_n or $HSC_{11}BIPY$) is the molar concentration of compound A.

The formation of binary SAMs was confirmed by X-ray photoelectron spectroscopy (XPS; see the Supporting Information for XPS spectra). The mole fraction of $HSC_{11}BIPY$ in solution ($\chi^{soln}_{HSC11BIPY}$) was translated to that on surface ($\chi^{surf}_{SC11BIPY}$) (Figure 1 d). The relation between $\chi^{soln}_{HSC11BIPY}$ and $\chi^{surf}_{SC11BIPY}$ was not perfectly linear. As the concentration of $HSC_{11}BIPY$ in solution increased, its preferential adsorption was observed for the mole fractions of $HSC_{11}BIPY$ below $\chi^{soln}_{HSC11BIPY} = 0.5$; the opposite adsorption behavior was observed for mole fractions above $\chi^{soln}_{HSC11BIPY} = 0.5$. This is attributed to the steric and electrostatic repulsions between polar and bulky BIPY groups,[13] which become noticeable as the ratio of $SC_{11}BIPY$ on surface increases beyond 50%.

Large-area junctions of binary SAMs were fabricated with Ga_2O_3/EGaIn conical tips following previously reported procedures.[5] Data of *J*–*V* traces were collected at ±1.0 V, and rectification ratio was calculated by using Equation (1) (see the Supporting Information for the histograms of $J(V)$ and r). The histograms of $J(V)$ and r for single-component SAMs typically exhibit log-normal distributions.[5,14] Mean and standard deviation were estimated from Gaussian curves

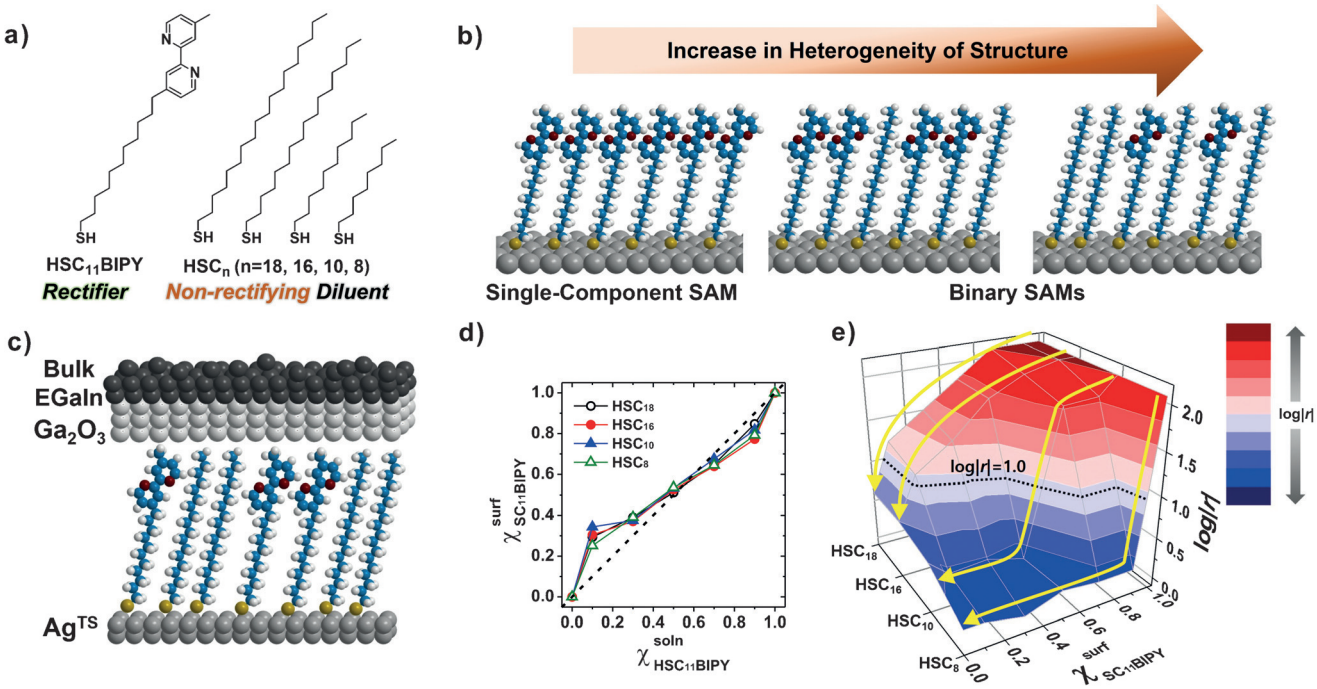

Figure 1. a) Molecules used to form single-component and binary SAMs for this study. $HSC_{11}BIPY$ is an organic rectifier, and HSC_n is non-rectifying *n*-alkanethiol used to dilute $SC_{11}BIPY$ SAM. b) Schematic representation of the increasing heterogeneity of the structure from a single-molecular component SAM to binary SAMs. Well-defined binary SAMs enable systematic dilution on a molecular scale. c) Structure of vertical metal–molecules–metal-oxide–metal junction of the form Ag^{TS}/SAM//Ga_2O_3/EGaIn used for measuring current density and rectification ratio (Ag^{TS} = template-stripped silver; Ga_2O_3/EGaIn = eutectic gallium-indium alloy covered with a surface film of Ga_2O_3). d) Relationship between mole fractions in solution ($\chi^{soln}_{HSC11BIPY}$) and on surface ($\chi^{surf}_{SC11BIPY}$; determined by XPS). The dashed line represents the case where $\chi^{soln}_{HSC11BIPY} = \chi^{surf}_{SC11BIPY}$. e) Trends of rectification ratio (mean of log-rectification ratio, $\log|r|_{mean}$) as a function of $\chi^{surf}_{SC11BIPY}$, and the length (*n* in the HSC_n) of *n*-alkanethiol diluent.

fit to histograms.[15] Histograms for SAMs comprising a mixture of rectifier and non-rectifying diluent have been rarely reported. Binary SAMs containing structural defects sufficient to affect $J(V)$ might yield r histograms exhibiting broad dispersion and/or significant outliers.

Figure 1e shows the trends of mean obtained from the histograms of $\log|r|$ ($\log|r|_{mean}$) as a function of $\chi^{surf}_{SC11BIPY}$ and the length of diluent (n in the HSC_n). Overall, the rectification ratio decreased with decreasing $\chi^{surf}_{SC11BIPY}$, confirming that rectification in the $Ag^{TS}/SC_{11}BIPY//Ga_2O_3/EGaIn$ junctions relies on the BIPY terminal unit rather than other asymmetric characteristics of the junction (e.g., asymmetric SAM-electrode contacts, and work functions of electrodes).[5] The magnitude of rectification ratio was finely tunable by control over the ratio of rectifier. Surprisingly, the gradient behavior of rectification for the long diluents (HSC_{16} and HSC_{18}) significantly differed from that for the short diluents (HSC_8 and HSC_{10}). Rectification for the binary SAMs diluted with the long chain length diluents maintained high r values ($\log|r|>1.0$) until around 90% of diluent was present on the surface (Figure 1e). In contrast, rectification disappeared when SAM was diluted with short HSC_n diluent. As HSC_n diluent was shortened, the points where $r=10$ ($\log|r|=1.0$ in ca. 10% and ca. 50% of HSC_8 and HSC_{10}, respectively, as shown in the Figure 1e) were moved further to $\chi^{surf}_{SC11BIPY}=1.0$.

We examined changes in the dispersion of r histograms through the trends of standard deviation ($\sigma_{\log|r|}$) and the ratio of outlier.[15] Overall, values of $\sigma_{\log|r|}$ for binary SAMs were higher than those for the corresponding single-component SAMs (see the histograms of r in the Supporting Information). Exceptionally small $\sigma_{\log|r|}$ were observed for the binary SAMs of the short diluents: e.g., $\chi^{soln}_{HSC11BIPY}=0.5$ for HSC_{10}; $\chi^{soln}_{HSC11BIPY}=0.7$ and 0.9 for HSC_8. These histograms showed significant tailing and peak splitting, which yielded large numbers of outliers. (Note that the similar feature was reported;[16] as the degree of structural defect for the SAM of ferrocene-terminated n-alkanethiolate rectifier increases, the histogram of r values increases exhibiting tailing and peak splitting.) Thus, we further estimated the ratio of the outlier bin-counts to total bin-counts (defined as outlier%) for the r histograms using the following equation, outlier% = (bin-count of outliers)/(total bin-count) × 100. We defined outlier bin-counts as those not lying within the range of $\log|r|_{mean} \pm 2\times\sigma_{\log|r|}$ (the range covers 95% of the bin-counts).[17] Figure 2 shows the trends of outlier%. We found that, overall, the histograms of binary SAMs exhibited more outliers than those of the corresponding single-component SAMs, and, the outlier% for the short diluents was higher than that for the long diluents. This is presumably due to significant amount of phase-separated domains in the binary SAMs of short diluents, resulting from weak lateral interactions between structurally largely different diluent and rectifier. In contrast, the thiol species that are similar in length (i.e., HSC_{18} and $HSC_{11}BIPY$) can avoid, at least in part, phase separation and form binary SAMs with relatively uniform composition. Indeed, the dependence of degree of phase separation for binary SAMs of n-alkanethiols on their difference in length has been well established in Ref. [18].

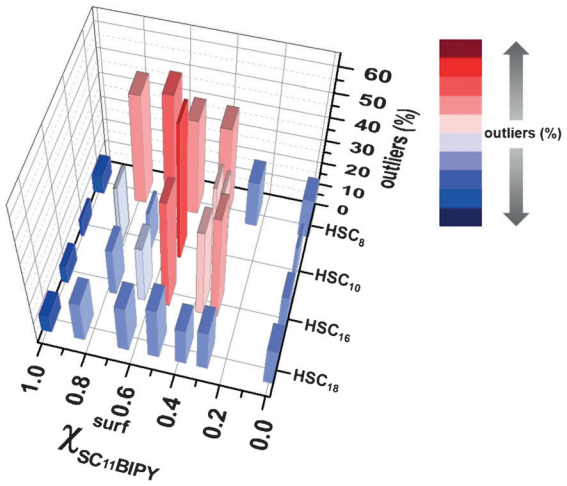

Figure 2. Outlier% (the ratio of the outlier bin-counts to total bin-counts; see text for details) plotted against $\chi^{surf}_{SC11BIPY}$ for different diluents (HSC_n; $n=8$, 10, 16, and 18).

Gradient of structural defect in the binary SAMs was further probed through static water contact angle goniometry and wet electrochemical analysis. Figure 3a summarizes the data of contact angle measurements. Upon the dilution of the $SC_{11}BIPY$ SAM with the long HSC_n diluents (HSC_{18} and HSC_{16}), the wettability of SAM surface decreased (see the orange-color arrow in Figure 3a): e.g., contact angle (θ) increased by a factor of about 1.5 when $\chi^{surf}_{SC11BIPY}$ changed from 1.0 to around 0.7. In contrast, opposite trend was observed for the short HSC_n diluents (HSC_{10} and HSC_8): the value of θ for

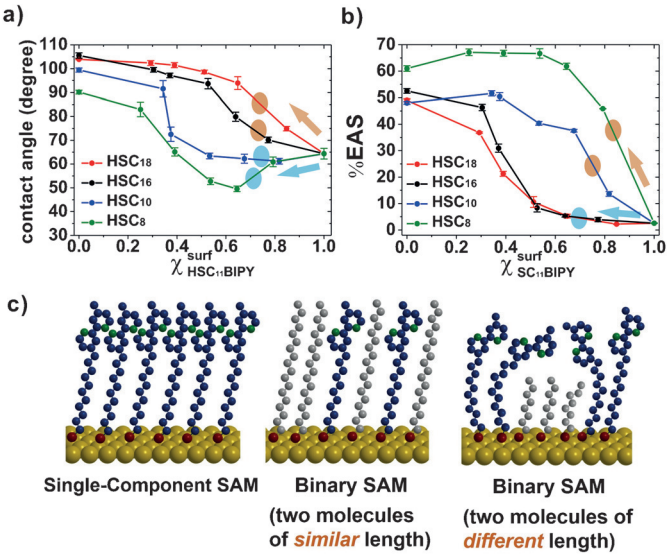

Figure 3. a) Measurements of static water contact angle for a series of single-component and binary SAMs formed with $HSC_{11}BIPY$ and HSC_n. See text for details. b) Data of wet electrochemical analysis of SAMs on gold (Au^{TS}) with 1 mM $Ru(NH_3)_6^{3+}$ as a redox probe in 0.1 M KCl solution. Values of %EAS (percent electrochemically active surface area) were measured for relative comparison of the degree of structural defect among SAMs. c) Schematic description of the tunability of structural defect of monolayers by controlling the structural difference between electronically active molecule (blue) and diluent (gray).

$\chi^{surf}_{SC11BIPY} \approx 0.7$ was a factor of around 1.3 smaller than that for $\chi^{surf}_{SC11BIPY} = 1.0$ (see the blue arrow in Figure 3a). SAMs were also analyzed by the measurements of %EAS (percent electrochemically active surface area).[19] A key idea underlying %EAS is that the surface coverage of SAM can be approximated by measuring the ratio of peak reduction currents for a SAM-bound electrode to the corresponding bare electrode. Therefore, %EAS enables relative comparison of the degree of structural defect between SAMs. Substantial defects in SAMs give high %EAS values, whereas low %EAS values imply tightly packed molecules on surfaces and low degree of defects in monolayers. To guarantee reliable measurements of %EAS, SAMs were formed on gold (Au^{TS}), which is electrochemically inert during wet electrochemical analysis. It was assumed that there is no significant difference between SAMs on Au and Ag for examining the *trends* of structural defect over SAMs. Indeed, the insensitivity of rectification for SC_{11}BIPY SAM to any changes in work function, tilt angle and packing density resulting from replacement of silver with gold was previously reported.[5] (This insensitivity may be peculiar to the BIPY-based rectifier; ferrocene-based rectifier previously exhibited the sensitivity of its rectification to changes in work function and tilt angle.[20]) Data of %EAS is shown in Figure 3b. Structural defects remarkably increased upon dilution with the short HSC_n diluents (see the orange arrow in Figure 3b), whereas slight change in %EAS was observed for the long HSC_n diluents (see the blue arrow in Figure 3b). Figure 3c shows a schematic to explain the observed strikingly different behaviors in the wettability and %EAS between the long and short diluents. The molecular-scale control over the structure of diluent yields the different gradients of rectification for different diluents.

We further determined whether the gradient of rectification could be achieved in the narrow window between $\chi^{soln}_{HSC11BIPY} = 1.0$ and 0.9 for binary SAMs of HSC_8 (as shown in Figure 1e). Surprisingly, the rectification ratio and %EAS concomitantly decreased and increased, respectively, as $\chi^{soln}_{HSC11BIPY}$ decreased from 0.999 (0.1% dilution) to 0.95 (5% dilution; Figure 4). This finding indicates that the rectification gradient of SC_{11}BIPY SAM can be tuned with extremely small amounts of short diluent. Indeed, Figure 4 shows that 1% dilution ($\chi^{soln}_{HSC11BIPY} = 0.99$) with HSC_8 leads to approximately one order of magnitude decrease in r, and rectification disappears upon 3% dilution ($\chi^{soln}_{HSC11BIPY} = 0.97$). The ultra-sensitivity of rectification to molecular dilution was valid for only the short HSC_8 molecule among the tested diluents. This finding implies that the effect of molecular dilution on the performance of SAM-based devices substantially depends on the molecular structure of diluent.

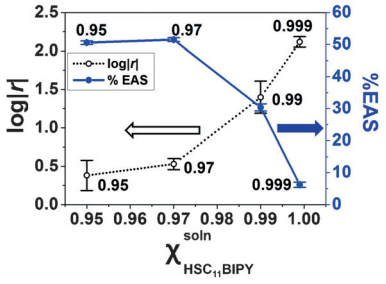

Figure 4. Plot of $\log|r|_{mean}$ and %EAS against $\chi^{soln}_{HSC11BIPY}$ for binary SAMs of HSC_8 within the particular range from $\chi^{soln}_{HSC11BIPY} = 1.0$ to 0.9. Ultra-sensitivity of the gradient of rectification to the HSC_8 dilution was observed.

In summary, we investigated the detailed electrical behavior of binary SAMs composed of organic rectifier, SC_{11}BIPY, and non-rectifying *n*-alkanethiolate diluents as a function of ratio of diluent on the surface and of the molecular structure of diluent. EGaIn-based junctions formed with well-defined binary SAMs enable highly tunable gradients of rectification based on the statistically significant data of *J*–*V* traces. The magnitude of rectification ratio varies over the range of approximately 10^2, without changing the polarity of rectification. As the ratio of diluent increases, the magnitude of rectification ratio decreases. This finding confirms that the rectification observed in Ag^{TS}/SC_{11}BIPY//Ga_2O_3/EGaIn junctions arises from asymmetrically positioned BIPY terminal moiety in the *n*-alkane backbone, not from any of asymmetric structures in junctions.[5] This study also establishes the molecular-scaling of diluents. Remarkably, the gradient behavior of rectification is finely tunable by controlling the structure (the molecular length) of the diluent relative to rectifier. The results reported in this study offer a method to modulate rectification by creating gradients with existing rectifiers, avoiding efforts to search new rectifiers.

The influence of structural disorder of SAMs on the performance of rectification in SAM-based junction has been reported.[1d] This previous work demonstrated that the rectification of SAMs formed with ferrocene-terminated *n*-alkanethiol disappears in the presence of the analogous disulfide impurity. However, we show that gradients of rectification ratio can be achieved by systematic dilution of the SAM, and the trend of rectification ratio against the degree of molecular dilution largely depends on the difference in length between rectifier and diluent. A further study to develop a theoretical model and rationalize detailed basis of gradients of rectification ratio is underway.

Acknowledgements

This research was supported by the Basic Science Research Program through the NRF of Korea funded by the Ministry of Science, ICT, & Future Planning (NRF-2014R1A1A1002938) and the Ministry of Education (NRF20100020209).

Keywords: dilution effects · EGaIn junctions · molecular electronics · rectifiers · self-assembled monolayers

How to cite: *Angew. Chem. Int. Ed.* **2016**, *55*, 10307–10311
Angew. Chem. **2016**, *128*, 10463–10467

[1] a) R. Mainz, E. S. Sanli, H. Stange, D. Azulay, S. Brunken, D. Greiner, S. Hajaj, M. D. Heinemann, C. A. Kaufmann, M. Klaus, Q. M. Ramasse, H. Rodriguez-Alvarez, A. Weber, I. Balberg, O. Millo, P. A. v. Aken, D. Abou-Ras, *Energy Environ. Sci.* **2016**, *9*, 1818–1827; b) C. Becher, L. Maurel, U. Aschauer, M. Lilienblum, C. Magén, D. Meier, E. Langenberg, M. Trassin, J. Blasco,

I. P. Krug, P. A. Algarabel, N. A. Spaldin, J. A. Pardo, M. Fiebig, *Nat. Nanotechnol.* **2015**, *10*, 661 – 665; c) W. Chen, Y. Wu, Y. Yue, J. Liu, W. Zhang, X. Yang, H. Chen, E. Bi, I. Ashraful, M. Grätzel, L. Han, *Science* **2016**, *350*, 944 – 948; d) L. Jiang, L. Yuan, L. Cao, C. A. Nijhuis, *J. Am. Chem. Soc.* **2014**, *136*, 1982 – 1991.

[2] a) R. C. Chiechi, E. A. Weiss, M. D. Dickey, G. M. Whitesides, *Angew. Chem. Int. Ed.* **2008**, *47*, 142 – 144; *Angew. Chem.* **2007**, *119*, 148 – 150; b) F. C. Simeone, H. J. Yoon, M. M. Thuo, J. R. Barber, B. Smith, G. M. Whitesides, *J. Am. Chem. Soc.* **2013**, *135*, 18131 – 18144.

[3] A. Aviram, M. A. Ratner, *Chem. Phys. Lett.* **1974**, *29*, 277 – 283.

[4] W. F. Reus, M. M. Thuo, N. D. Shapiro, C. A. Nijhuis, G. M. Whitesides, *ACS Nano* **2012**, *6*, 4806 – 4822.

[5] H. J. Yoon, K.-C. Liao, M. R. Lockett, S. W. Kwok, M. Baghbanzadeh, G. M. Whitesides, *J. Am. Chem. Soc.* **2014**, *136*, 17155 – 17162.

[6] E. A. Weiss, G. K. Kaufman, J. K. Kriebel, Z. Li, R. Schalek, G. M. Whitesides, *Langmuir* **2007**, *23*, 9686 – 9694.

[7] C. A. Nijhuis, W. F. Reus, J. R. Barber, M. D. Dickey, G. M. Whitesides, *Nano Lett.* **2010**, *10*, 3611 – 3619.

[8] a) R. K. Smith, S. M. Reed, P. A. Lewis, J. D. Monnell, R. S. Clegg, K. F. Kelly, L. A. Bumm, J. E. Hutchison, P. S. Weiss, *J. Phys. Chem. B* **2001**, *105*, 1119 – 1122; b) L. J. C. Jeuken, N. N. Daskalakis, X. Han, K. Sheikh, A. Erbe, R. J. Bushby, S. D. Evans, *Sens. Actuators B* **2007**, *124*, 501 – 509; c) L. Patrone, V. Gadenne, S. Desbief, *Langmuir* **2010**, *26*, 17111 – 17118.

[9] S.-H. Hsu, D. N. Reinhoudt, J. Huskens, A. H. Velders, *J. Mater. Chem.* **2011**, *21*, 2428 – 2444.

[10] J. H. Kim, H. S. Shin, S. B. Kim, T. Hasegawa, *Langmuir* **2004**, *20*, 1674 – 1679.

[11] S. D. Evans, E. Urankar, A. Ulman, N. Ferris, *J. Am. Chem. Soc.* **1991**, *113*, 4121 – 4131.

[12] a) B. L. Kropman, D. H. A. Blank, H. Rogalla, *Langmuir* **2000**, *16*, 1469 – 1472; b) R. S. Clegg, S. M. Reed, R. K. Smith, B. L. Barron, J. A. Rear, J. E. Hutchison, *Langmuir* **1999**, *15*, 8876 – 8883; c) C. J. V. Oss, M. K. Chaudhury, R. J. Good, *Chem. Rev.* **1988**, *88*, 927 – 941.

[13] H. J. Lee, A. C. Jamison, T. R. Lee, *Acc. Chem. Res.* **2015**, *48*, 3007 – 3015.

[14] C. A. Nijhuis, W. F. Reus, G. M. Whitesides, *J. Am. Chem. Soc.* **2009**, *131*, 17814 – 17827.

[15] W. F. Reus, C. A. Nijhuis, J. R. Barber, M. M. Thuo, S. Tricard, G. M. Whitesides, *J. Phys. Chem. C* **2012**, *116*, 6714 – 6733.

[16] L. Yuan, L. Jiang, D. Thompson, C. A. Nijhuis, *J. Am. Chem. Soc.* **2014**, *136*, 6554 – 6557.

[17] G. D. Kong, M. Kim, H. J. Yoon, *J. Electrochem. Soc.* **2015**, *162*, H703 – H712.

[18] a) K. Tamada, M. Hara, H. Sasabe, W. Knoll, *Langmuir* **1997**, *13*, 1558 – 1566; b) P. E. Laibinis, R. G. Nuzzo, G. M. Whitesides, *J. Phys. Chem.* **1992**, *96*, 5097 – 5105; c) J. P. Folkers, P. E. Laibinis, G. M. Whitesides, *Langmuir* **1992**, *8*, 1330 – 1341.

[19] M. H. Schoenfisch, J. E. Pemberton, *J. Am. Chem. Soc.* **1998**, *120*, 4502 – 4513.

[20] a) L. Yuan, D. Thompson, L. Cao, N. Nerngchangnong, C. A. Nijhuis, *J. Phys. Chem. C* **2015**, *119*, 17910 – 17919; b) P. Song, L. Yuan, M. Roemer, L. Jiang, C. A. Nijhuis, *J. Am. Chem. Soc.* **2016**, *138*, 5769 – 5772.

Received: May 16, 2016
Revised: June 24, 2016
Published online: July 22, 2016

